Original Investigation

The Endoscopic Endonasal Approach to the Hypoglossal Canal
The Role of the Eustachian Tube as a Landmark for Dissection

Satyan B. Sreenath, MD; Pablo F. Recinos, MD; Stanley W. McClurg, MD; Brian D. Thorp, MD; Kibwei A. McKinney, MD; Cristine Klatt-Cromwell, MD; Adam M. Zanation, MD

IMPORTANCE Improvements in endoscopic technology and reconstructive techniques have made the endoscopic endonasal approach (EEA) a viable option to approach ventromedial lesions in the region of the hypoglossal canal. Prior to contemplating this surgical corridor, a thorough understanding of anatomic relationships and landmarks is essential to safely approach this region of the posterior skull base through an EEA.

OBJECTIVE To describe the surgical technique and anatomic landmarks in the EEA to the hypoglossal canal through referencing nasopharyngeal and posterior skull base anatomy.

DESIGN, SETTING, AND PARTICIPANTS Study of latex-injected cadaveric heads at the North Carolina Eye Bank Multidisciplinary Surgical Skills Laboratory at the University of North Carolina.

INTERVENTIONS An EEA to the hypoglossal canal was carried out bilaterally in 5 embalmed, latex-injected cadaver heads.

MAIN OUTCOMES AND MEASURES Cadaveric measurements of anatomic landmarks and relationships in the approach were obtained using a 10-cm surgical ruler and were reported as mean distances. Additionally, high-quality endoscopic images demonstrating the operative technique and anatomic relationships were obtained.

RESULTS The distance between the lacerum segment of the internal carotid arteries, the superolateral boundary, was 23.6 mm (SD, 11.8 mm). The distance between the anterolateral edge of the occipital condyles, the inferolateral boundary, was 19 mm (SD, 0.80 mm). The supracondylar groove was identified in the same anteroposterior plane as the nasopharyngeal orifice of the eustachian tube, and the anterior-most edge of the occipital condyle was 14 mm (SD, 0.82 mm) from the posterosuperior edge of the salpingopharyngeal fold. Additionally, the transtubercular corridor was on the same plane as the superior edge of the torus tubarius in the anteroposterior axis. The distance to the hypoglossal canal from midline was 10 mm, which was found after completing drilling in the transcondylar and transtubercular corridors. Last, the hypoglossal nerve rootlets were identified entering the canal 6 mm inferiorly and 8 mm laterally from the vertebrobasilar junction.

CONCLUSIONS AND RELEVANCE The eustachian tube and other elements of nasopharyngeal anatomy are fixed landmarks that provide important points of reference when approaching the hypoglossal canal through an EEA. A thorough understanding of these anatomic relationships is vital in safely navigating this direct, surgical corridor to the posterior fossa.

JAMA Otolaryngol Head Neck Surg. 2015;141(10):927-933. doi:10.1001/jamaoto.2015.1749
Published online September 17, 2015.

Author Affiliations: Department of Otolaryngology–Head and Neck Surgery, University of North Carolina at Chapel Hill, Chapel Hill (Sreenath, McClurg, Thorp, McKinney, Klatt-Cromwell, Zanation); Department of Neurosurgery, University of North Carolina at Chapel Hill, Chapel Hill (Recinos, Zanation); Rosa Ella Burkhardt Brain Tumor and Neuro-Oncology Center, Cleveland Clinic, Cleveland, Ohio (Recinos); Head and Neck Institute, Cleveland Clinic, Cleveland, Ohio (Recinos).

Corresponding Author: Adam M. Zanation, MD, Departments of Otolaryngology–Head & Neck Surgery and Neurosurgery, University of North Carolina at Chapel Hill, 170 Manning Dr, CB #7070, Physician's Office Bldg, Rm G-190, Chapel Hill, NC 27599 (adam_zanation@med.unc.edu).

The hypoglossal canals are paired channels in the occipital bone that transmit cranial nerve (CN). The intracranial, intradural orifice of the hypoglossal canal is located on the medial surface of the occipital condyle, with the extracranial orifice opening into the parapharyngeal space on the lateral surface of the occipital condyle.[1-3] Lesions involving the hypoglossal canal are rare but can include schwannomas, clival chordomas, petroclival meningiomas, jugulotympanic paragangliomas, or metastases.[1,4] Transcranial approaches have been the standard operative approaches in managing these lesions, including the modified Fisch type A infratemporal fossa approach, the supracondylar approach, the extended posterolateral approach, the far-lateral approach (with transcondylar and/or transtubercular extensions), and the transjugular craniotomy.[4-9] However, when a lesion involving the hypoglossal canal is located on the ventral surface of the brainstem or in the anterior aspect of the lower clivus, access to these tumors through traditional approaches can often result in manipulation of the lower cranial nerves, vascular structures, and the brainstem. This can be associated with high clinical morbidity and complications such as CNs X and XI palsies.[10,11] Benet et al[12] divided the surfaces of the brainstem into the ventromedial and dorsolateral compartments, which were defined as the spaces anterior and posterior to CNs VII through XII, respectively. Although the lateral, transcranial approaches are the primary accepted surgical options in approaching lesions in the dorsolateral compartment, there is no standard method for approaching lesions of the ventromedial compartment.[13-15]

With continued improvements in endoscopic technologies and reconstructive techniques, the expanded role of endoscopic endonasal approaches (EEAs) has changed the operative paradigm in managing tumors of the middle and posterior skull base.[11,16-18] In 2010, Morera et al[19] first described the far-medial EEA to the inferior third of the clivus, with lateral extension via the transcondylar and transtubercular approach to the hypoglossal canal. In this cadaveric study, an approach to the hypoglossal canal through a lateral extension of the inferior endoscopic endonasal transclival approach was described.[19] Of note, they described the *supracondylar groove*, an area on the superior surface of the occipital condyle formed by the insertion of the rectus capitus anterior muscle, anterior atlantooccipital membrane, and atlantooccipital capsule joint. This groove was proposed as a reliable anatomic landmark for estimating the position of the hypoglossal canal and its external opening, which is immediately posterior and lateral to the groove, respectively.[19] Since the supracondylar groove was identified and proposed as a reliable anatomic landmark, this approach to the inferior clival region and hypoglossal canal has been anatomically studied in a comparative analysis of the far-medial EEA and far-lateral transcranial, transcondylar approaches to the inferolateral clival region and craniovertebral junction, which confirmed initial reports that the far-medial endoscopic approach is an ideal operative technique for lesions ventromedial to the brainstem.[12] Additionally, the EEA approach to the inferior clival region has been successfully described in vivo in the management of a chordoma involving the inferior clivus, occipital condyle, and jugular tubercle.[12,20] However, given the novelty of this approach, the nuances of the operative corridor and surgical landmarks continue to be refined and characterized.

In this study, we postulated that sinonasal and nasopharyngeal anatomy could act as useful reference points in the endoscopic endonasal and far-medial approaches to the posterior skull base and craniovertebral junction. Through cadaveric dissection, we sought to further define the endoscopic endonasal approach to the hypoglossal canal while referencing nasopharyngeal and posterior skull base anatomy. We hypothesized that by using more anterior structures in this surgical window, such as the eustachian tube, consistent landmarks could be identified with successive progression posteriorly to assist in dissection of the inferolateral clival region and craniovertebral junction.

Methods

Anatomical Dissection Specimens and Endoscopic Equipment

Five latex-injected cadaver heads were obtained for the anatomical study, which was conducted in the North Carolina Eye Bank Multidisciplinary Surgical Skills Laboratory at the University of North Carolina. Endoscopic, endonasal dissections were carried out using 0° and 45° rigid rod–lens endoscopes (Stryker Corp), which were connected to an LED light source and a high-definition endoscopic camera (Stryker Corp). Endoscopic sinonasal and skull base surgical instruments (Medtronic), high-speed 3.0- and 4.0-mm diamond and cutting burrs (Stryker Corp), and a suction microdebrider (Stryker Corp) were used for the cadaver dissection. Cadaveric measurements were obtained using a 10-cm surgical ruler.

The University of North Carolina institutional review board approved this study.

Exposure in the EEA to the Middle and Inferior Clivus

Exposure consistent with standard EEAs was obtained in the sinonasal cavity to allow for a bimanual dissection, which has been well described.[16,21-25] Bilateral dissection to the hypoglossal canal was performed in each of the 5 heads. First, the endoscope was advanced into the right nasal passage, immediately visualizing the right inferior and middle turbinates and nasal septum. The right middle turbinate was resected using turbinate scissors to increase instrument maneuverability. Next, to increase lateral exposure, a routine uncinectomy and ethmoid bullectomy were performed, which allowed visualization of the natural ostium of the maxillary sinus. Next, a complete anterior and posterior ethmoidectomy was performed, with wide exposure of the ethmoid roof and lamina papyracea. The sphenoid ostium was then identified on the right side, and a wide sphenoidotomy was performed. The endoscope was then advanced into the left nasal passage where the same steps were performed. The posterior septum was then disarticulated from the rostrum of the sphenoid bone, and the posterior 2 cm of the nasal septum was resected down to the hard palate. At this point, a wide surgical corridor was created, facilitating bilateral instrumentation via the 2- surgeon, 4-handed technique for the remainder of the dissection.[26]

Figure 1. Nasopharyngeal Dissection to the Craniovertebral Junction

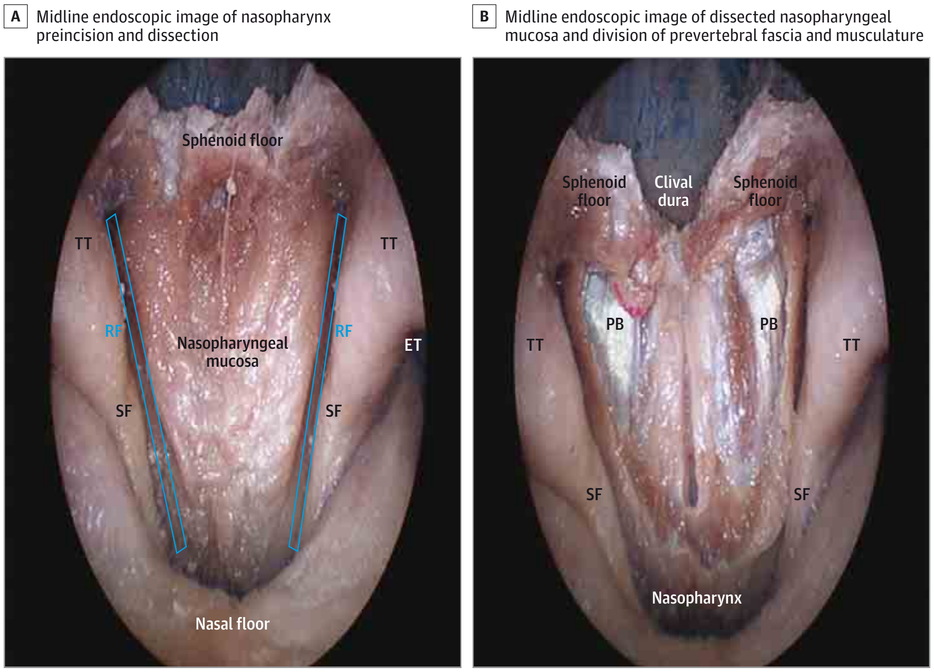

Photographs A and B show the dissection of nasopharyngeal and prevertebral fascia and musculature in approaching the inferior clival region and craniovertebral junction. SF indicates salpingopharyngeal fold; RF, Rosenmüller's fossa; ET, eustachian tube; TT, torus tubarius; PB, pharyngobasilar fascia.

Next, attention was turned toward identification of the bilateral paraclival and lacerum segments of the internal carotid artery (ICA), as the lacerum ICA represents the superolateral limit of the EEA to the hypoglossal canal.[19,27] First, the vidian nerve was located, since it is a known landmark for locating the petrous ICA and lacerum ICA.[28] The vidian canal was identified by locating the intersection of the inferior and lateral walls of the sphenoid sinus with the medial pterygoid plate. The medial pterygoid plate leads to the pterygoid wedge, in which the vidian canal is centrally located.[28] The bone inferomedial to the vidian canal was then drilled bilaterally. This bone protects the vidian nerve and allows for safe exposure of the lacerum portion of the ICA. The paraclival segments of the ICA were also skeletonized to verify their location and prevent inadvertent injury. After achieving exposure of the superolateral boundaries of the approach to the hypoglossal canal, attention was turned to dissection of the posterior nasopharynx and inferior clivus.

With the lacerum segments of the ICA exposed, the remainder of the inferior wall of the sphenoid sinus was drilled back until it was flush with the clivus. A midline incision was made in the nasopharyngeal mucosa and musculature, which was resected or reflected laterally, exposing the pharyngobasilar fascia while avoiding injury to the eustachian tubes laterally (**Figure 1**). The pharyngobasilar fascia was resected from its attachments to the inferior clivus, revealing the longus capitus, rectus capitus anterior, and the atlantooccipital membrane, which were all resected or reflected laterally (Figure 1). Now, the anterior ring of C1, atlantooccipital joint capsules, and alar ligament are visualized (**Figure 2**). From the level of the lacerum segments of the ICA, the inferior clivus, medial to these structures, was drilled down using a 4.0-mm diamond burr until clival dura was exposed, ensuring not to violate the dural plane (Figure 2).

Approach to the Hypoglossal Canal Through Referencing the Eustachian Tube

At this point, the inferior clivus, foramen magnum, and atlantooccipital joint capsule were exposed. To better identify bony landmarks, the suction microdebrider (Stryker Corp) was used to remove excess soft tissue and open the atlantooccipital joint capsule bilaterally. The supracondylar groove was identified bilaterally based on descriptions provided by Morera et al[19] (Figure 2). Next, the transtubercular compartment in the jugular tubercle was identified as laying in the same plane as the superior edge of the torus tubarius in the anteroposterior axis (**Figure 3**). Last, the transcondylar compartment was identified based on the ventral surface of the occipital condyle. With clear anatomic boundaries of these compartments, the transtubercular compartment followed by the transcondylar compartment was drilled using a 4.0-mm diamond burr (Stryker Corp). Both compartments were drilled in a posterior to anterior direction to minimize the risk of slipping into the neurovascular plane immediately posterior to these compartments (**Figure 4**). The hypoglossal canal and its external opening were visualized from a superior and inferior aspect once the drilling was complete (Figure 4).

Intradural Exploration of Vertebrobasilar Anatomy and the Hypoglossal Nerve

The dissection proceeded posteriorly to reveal the retroclival, intradural anatomy of the vertebrobasilar system, and the lower cranial nerves. An incision was made in a posterior to anterior direction in the inferior clival dura, which was subsequently opened, revealing the vertebral arteries, vertebrobasilar junction (VBJ), basilar artery, and lower cranial nerves. Clival dura was resected using Kerrison rongeurs. The intradural component of the hypoglossal nerve rootlets was iden-

Figure 2. Sinonasal, Clival, and Craniovertebral Junction Exposure

A Midline endoscopic image of nasopharyngeal dissection and skull base resection prior to dural incision

B Midline endoscopic image of nasopharyngeal dissection and exposure of vertebro basilar junction

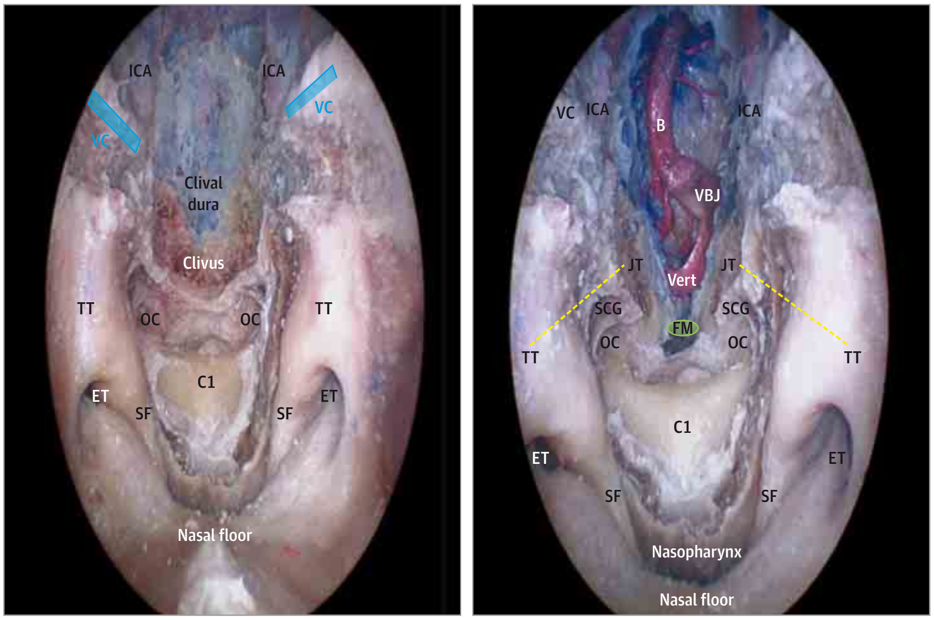

With complete resection of the sphenoid sinus floor, full visualization of the middle and inferior clivus can be obtained. After total nasopharyngeal dissection, the craniovertebral junction can be appreciated. ET indicates eustachian tube; SF, salpingopharyngeal fold; TT, torus tubarius; OC, occipital condyle; C1, first cervical spine bone; ICA, internal carotid artery; B, basilar artery; VBJ, vertebrobasilar junction; Vert, vertebral artery; SCG, supracondylar groove; VC and blue rectangles, Vidian canal; and FM and green circle, foramen magnum.

Figure 3. Surgical Window and Anatomic Landmarks

A Endoscopic image of trapezoidal surgical window

B Endoscopic image (45°) of relationships between nasopharyngeal and posterior skull base structures

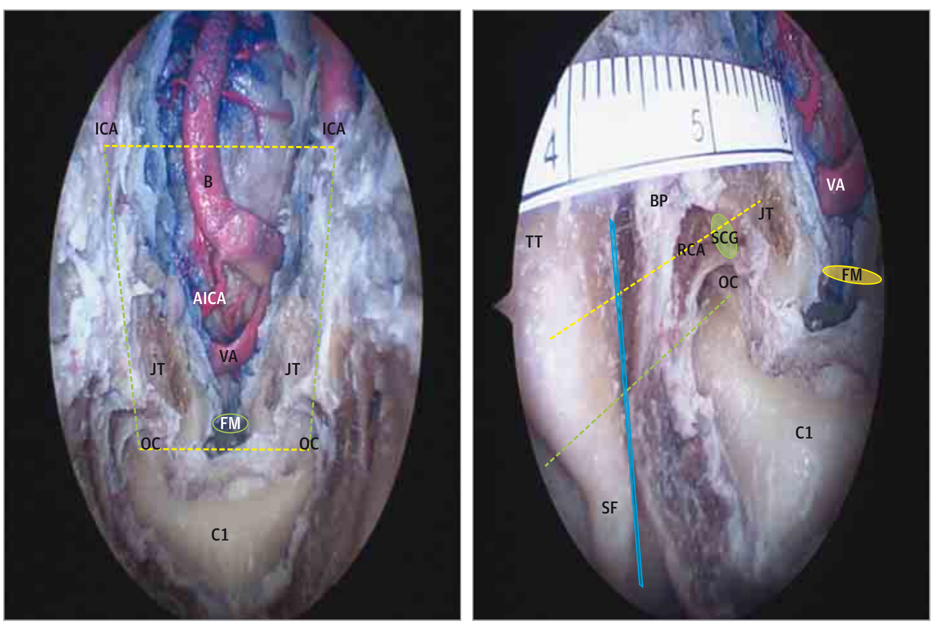

A, Endoscopic image demonstrating the trapezoidal surgical window and critical anatomic landmarks in approaching the hypoglossal canal from an endoscopic endonasal approach. B, Demonstration of relationships between nasopharyngeal structures and posterior skull base structures with the use of a 45° nasal endoscope. ICA indicates internal carotid artery; B, basilar artery; AICA, anterior inferior cerebellar artery; VA, vertebral artery; JT, jugular tubercle; OC, occipital condyle; FM, foramen magnum; C1, first cervical spine bone; SF, salpingopharyngeal fold; BP, basopharyngeal fascia; RCA, rectus capitus anterior muscle; blue rectangle, Rosenmüller's fossa; SCG and green circle, supracondylar groove; and FM and yellow circle, foramen magnum.

tified arising from the preolivary sulcus and passing behind the vertebral artery then entering the hypoglossal canal (Figure 4). The bilateral abducens nerves were identified arising from the pontomedullary junction and traveling anteriorly to pierce dura and enter the Dorello canal. Using a 45° nasal endoscope, visualization of the lateral borders of the premedullary cistern was obtained and CN IX, X, and XI were identified traveling into the jugular foramen.

Results

Understanding the Limits of Exposure in the EEA to the Middle and Inferior Clivus

Initially, we created a trapezoidal surgical window that was wider superiorly and narrower inferiorly (Figure 3). Defining the superolateral border of the approach, the mean distance be-

Figure 4. Exposure of the Hypoglossal Nerve and Canal

A Endoscopic image (45°) of hypoglossal nerve rootlets entering the hypoglossal canal

B Endoscopic image of 2 approaches to the hypoglossal canal

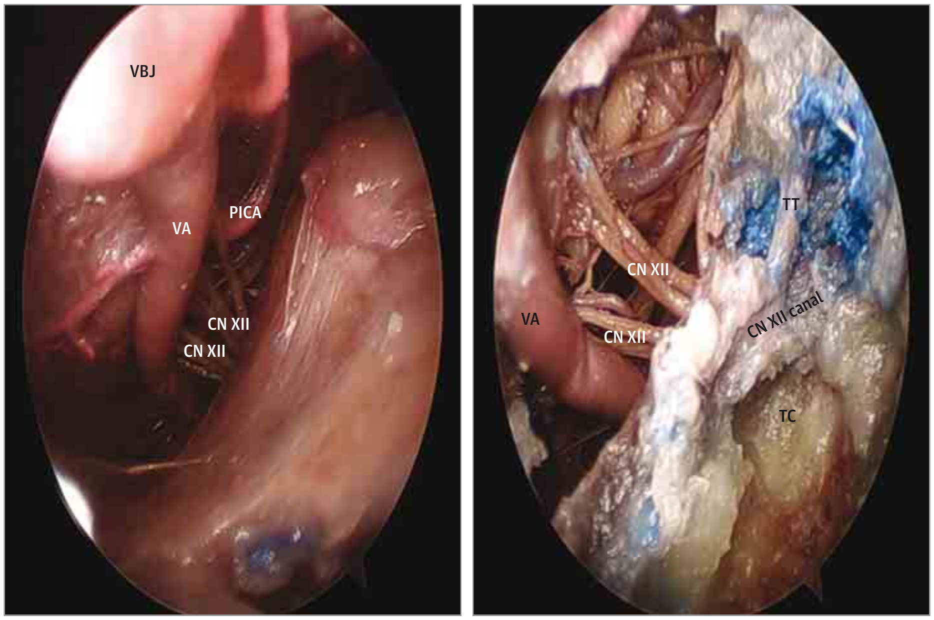

A, Intradural exposure of the hypoglossal nerve rootlets (cranial nerve XII) entering the hypoglossal canal through the view of a 45° nasal endoscope. B, Demonstration of the transcondylar and transtubercular approaches to the hypoglossal canal (cranial nerve XII). VBJ indicates vertebrobasilar junction; VA, vertebral artery; PICA, posterior inferior cerebellar artery; CN XII, cranial nerve XII (hypoglossal nerve); TT, transtubercular approach; TC, transcondylar approach.

tween the lacerum segments of the ICA was 23.6 mm (SD, 11.8 mm) (**Table**). Defining the inferolateral border of the approach, the mean distance between the anterior-most edges of the occipital condyles was 19 mm (SD, 0.80 mm). The mean distance between the nasopharyngeal orifices of the eustachian tubes was 19.6 mm (SD, 3.29 mm). Next, distances in the vertical axis were defined. The average distance from the floor of the sphenoid sinus to the ring of the C1 bone was 32.8 mm (SD, 6.07 mm). Last, the average height from the nasal floor to the superior aspect of the torus tubarius was 13 mm (SD, 2.5 mm).

The Eustachian Tube as a Landmark for Dissection

The supracondylar groove was related in the anterior-posterior plane to the eustachian tube orifice in the nasopharynx, where the distance between these structures on the anterior-posterior axis was 26 mm (SD, 1.4 mm) (Figure 3). From midline, identified as a plane perpendicularly bisecting the sphenoid rostrum anteriorly and basion posteriorly, the distance to the superomedial edge of the torus tubarius was 9.8 mm (SD, 2.8 mm). Progressing posteriorly, the distance from the posterosuperior edge of the salpingopharyngeal fold to the anterior-most edge of the occipital condyle was 13.8 mm (SD, 0.82 mm) (Table). Prior to drilling in the region of the hypoglossal canal, it was determined that the superior edge of the torus tubarius lay in the same plane in the anteroposterior axis as the jugular tubercle, thus demonstrating where to drill in the transtubercular approach to the hypoglossal canal (Figure 3).[19] Last, once both approaches to the canal were completed, the average distance between the intradural openings of the hypoglossal canals was 19.2 mm (SD, 5.5 mm).

Landmarks for Retroclival Intradural Exploration

First, the average height of the vertebrobasilar junction (VBJ) above the foramen magnum was determined to be 21.6 mm (SD, 4.92 mm) (Table). From the VBJ, the hypoglossal nerve rootlets pierced the canal approximately 6 mm inferiorly and 8 mm laterally. Although difficult to quantify, the hypoglossal nerve rootlets passed directly posterior to the vertebral artery and are in close proximity to the posterior inferior cerebellar artery in the path to the canal. Additionally, the relationship of the abducens nerve to the VBJ was observed. From the VBJ, the mean distance to the origin of the abducens nerve was 3 mm inferiorly and 4 mm laterally.

Discussion

The hypoglossal nerve generally exits the brainstem as 2 nerve bundles that travel an average of 11 mm to enter the intradural opening of the hypoglossal canal, where they unite to form 1 nerve.[1,29] Lesions and other pathologies involving the hypoglossal canal, ventromedial region of the foramen magnum, and inferior clivus have been historically difficult to surgically manage given the proximity of other critical structures such as the ICA, vertebrobasilar circulation, and lower cranial nerves.[1] With the advent of the EEA, surgical access to tumors involving the ventral surface of the skull base was revolutionized and continues to progress as our understanding of the surgical anatomy and operative technique continues to improve.[11,16,17]

Anatomical References in the Operative Approach

In this study, we were able to successfully characterize the EEA to the hypoglossal canal through referencing anatomy of the nasopharynx and craniovertebral junction. First, through recording measurements of the operative window, we are able to understand the limits of exposure in this approach. This is particularly helpful when considering the relationship of the

Table. Cadaveric Anatomical Distance Measurements

Anatomical Distances	Distance, Mean (SD), mm
Between lacerum segment of internal carotid arteries	23.6 (11.8)
Between anterior edge of OC	19.0 (0.8)
From anterior aspect of the nasopharyngeal opening of the eustachian tube to the supracondylar groove	26.0 (1.4)
From salpingopharyngeal fold to anterior edge of OC	14.0 (0.82)
Vertebrobasilar junction above foramen magnum	21.6 (4.92)

Abbreviation: OC, occipital condyles.

operative window to the size of the intended lesion that is being approached. By considering the dimensions of the operative window, it is possible to extend this window superiorly as necessary into the middle clivus to assist in surgical resection. Conversely, with an idea of the area of the operative window, it can be determined whether staged resection or combined approach would be more appropriate.

Second, it was noted that the supracondylar groove, an osseous landmark previously established by Morera et al,[19] lay in the same plane as the superior edge of the nasopharyngeal orifice of the eustachian tube in the anteroposterior axis. By noting the average distance from the posterosuperior edge of the salpingopharyngeal fold to the occipital condyle in the anteroposterior axis, combined with the relationship of the eustachian tube opening to the supracondylar groove, we are able to fully relate the supracondylar groove to more anteriorly based structures. Additionally, it was identified that the superior limit of the torus tubarius lay in the same plane as the jugular tubercle on the anteroposterior axis, which is particularly important because this helps denote where drilling should occur for the transtubercular approach to the hypoglossal canal. Next, by noting the average distance of the intradural opening of the hypoglossal canal from both midline and the VBJ, we were able to determine an approximate lateral distance to guide in the drilling of the jugular tubercle to obtain view of the canal. Given the proximity of the jugular bulb and CNs IX through XI to the dorsal surface of the jugular tubercle, it is vital to use knowledge of the approximate distances to the hypoglossal canal, along with the assistance of neuronavigation and potentially Doppler and neural monitoring to prevent unintentional drilling through the jugular tubercle.

Third, we successfully identified the relationship of the VBJ to the foramen magnum and internal orifice of the hypoglossal canal. With these relationships in mind, we were able to identify where it was safer to open dura in the midline and minimize risk of injury to vascular structures of the vertebrobasilar system. Additionally, by identifying the distance of the internal orifice of the hypoglossal canal from the VBJ, we are able to denote the level of lateral exposure required to obtain view of the internal opening of the hypoglossal canal, a critical step in approaching lesions in the intradural, ventromedial compartment.

Clinical Considerations of the EEA to the Hypoglossal Canal

Historically, one of the most common complications of the EEA was the high rate of cerebrospinal fluid leaks. The rate of cerebrospinal fluid leaks has been dramatically reduced with the introduction of vascularized, pedicled flaps, including the nasoseptal flap.[11,30-34] However, there are additional biomechanical and vascular factors that must be considered prior to approaching the hypoglossal canal.

Biomechanically, there are implications of drilling the occipital condyle. Perez-Orribo et al[35] investigated the biomechanical implications of ventral resection of the occiptocondylar joint on the stability of the craniovertebral junction during endoscopic endonasal approaches to the posterior skull base. They concluded that craniocervical fusion is indicated in patients who undergo greater than 75% anterior condylectomy. Of note, this study[35] concluded that a larger degree of resection is acceptable from an anterior approach prior to considering craniocervical fusion compared with an earlier study[36] that concluded that craniocervical fusion is indicated in patients who undergo greater than 50% posterior condylectomy. In the study by Morera et al,[19] it was noted that in relation to the condyle, the hypoglossal canal lies at the midpoint of the condyle, meaning that no more than 50% of condylar resection is expected to achieve access to the canal. However, it has also been noted that there are significant differences in the dimensions of individual occipital condyles and locations of the hypoglossal canal. Given these differences, it is crucial to always preoperatively assess these characteristics on radiographic analysis.[2] Prior to attempting the EEA to the hypoglossal canal, it is important to understand the level of condylar resection that is expected and always consider the potential need for craniocervical fusion.

The vascular anatomy of the vertebrobasilar circulation must be well understood if the ventral approach to the hypoglossal canal will extend into the intradural compartment. In their study of computed tomographic angiograms, Ciappetta et al[37] demonstrated that the relationship of the jugular tubercle and the posterior inferior cerebellar artery varies significantly. Given that the occipital condyle and jugular tubercle lie close to the VBJ, their relationship can be further studied on preoperative computed tomographic angiography to avoid inadvertent vascular injury. Thus, it is crucial to appreciate the vascular anatomy before attempting the transtubercular approach in the EEA to the hypoglossal canal.

Last, it is important to emphasize that while this approach provides direct surgical access to the ventromedial brainstem and minimizes manipulation of the lower cranial nerves and vascular structures compared with traditional approaches, thorough understanding of the neurovascular anatomy in this location is critical to avoid devastating complications if these structures are inadvertently transgressed. Extensive preoperative planning and use of neuronavigation should be standard practice in these operative scenarios but should not supplant the surgeons' anatomic knowledge.

Conclusions

The EEA to the hypoglossal canal provides a direct corridor for approaching lesions involving both the hypoglossal canal and the ventromedial space of the lower, lateral clival region, and craniocervical junction. In approaching this region, anatomic references of the nasopharynx, such as the eustachian tube and torus tubarius, may provide useful reference points to identify the occipital condyle and jugular tubercle when creating corridors to the hypoglossal canal and inferolateral clivus.

ARTICLE INFORMATION

Submitted for Publication: April 17, 2015; final revision received June 19, 2015; accepted July 24, 2015.

Published Online: September 17, 2015. doi:10.1001/jamaoto.2015.1749.

Author Contributions: Drs McClurg and Thorp had full access to all of the data in the study and take responsibility for the integrity of the data and the accuracy of the data analysis.
Study concept and design: Sreenath, Recinos, McClurg, Zanation.
Acquisition, analysis, or interpretation of data: Sreenath, Recinos, McClurg, Thorp, McKinney, Klatt-Cromwell, Zanation.
Drafting of the manuscript: Sreenath, Zanation.
Critical revision of the manuscript for important intellectual content: Sreenath, Recinos, McClurg, Thorp, McKinney, Klatt-Cromwell, Zanation.
Statistical analysis: Sreenath, Recinos, McKinney.
Administrative, technical, or material support: Sreenath, Recinos, McClurg, Klatt-Cromwell, Zanation.
Study supervision: McClurg, Thorp, Zanation.

Conflict of Interest Disclosures: None reported.

Previous Presentation: This study was presented at the Fifth World Congress of the International Federation of Head and Neck Oncologic Societies and Annual Meeting of the American Head and Neck Society; July 30, 2014; New York, New York.

REFERENCES

1. Hadley KS, Shelton C. Infratemporal fossa approach to the hypoglossal canal: practical landmarks for elusive anatomy. *Laryngoscope*. 2004;114(9):1648-1651.

2. Naderi S, Korman E, Citak G, et al. Morphometric analysis of human occipital condyle. *Clin Neurol Neurosurg*. 2005;107(3):191-199.

3. Voyvodic F, Whyte A, Slavotinek J. The hypoglossal canal: normal MR enhancement pattern. *AJNR Am J Neuroradiol*. 1995;16(8):1707-1710.

4. Calzada G, Isaacson B, Yoshor D, Oghalai JS. Surgical approaches to the hypoglossal canal. *Skull Base*. 2007;17(3):187-196.

5. Fisch U, Pillsbury HC. Infratemporal fossa approach to lesions in the temporal bone and base of the skull. *Arch Otolaryngol*. 1979;105(2):99-107.

6. Gilsbach JM, Sure U, Mann W. The supracondylar approach to the jugular tubercle and hypoglossal canal. *Surg Neurol*. 1998;50(6):563-570.

7. Kratimenos GP, Crockard HA. The far lateral approach for ventrally placed foramen magnum and upper cervical spine tumours. *Br J Neurosurg*. 1993;7(2):129-140.

8. Myatt HM, Holland NJ, Cheesman AD. A skull base extradural hypoglossal neurilemmoma resected via an extended posterolateral approach. *J Laryngol Otol*. 1998;112(11):1052-1057.

9. Oghalai JS, Leung MK, Jackler RK, McDermott MW. Transjugular craniotomy for the management of jugular foramen tumors with intracranial extension. *Otol Neurotol*. 2004;25(4):570-579.

10. D'Ambrosio AL, Kreiter KT, Bush CA, et al. Far lateral suboccipital approach for the treatment of proximal posteroinferior cerebellar artery aneurysms: surgical results and long-term outcome. *Neurosurgery*. 2004;55(1):39-50.

11. Snyderman CH, Carrau RL, Kassam AB, et al. Endoscopic skull base surgery: principles of endonasal oncological surgery. *J Surg Oncol*. 2008;97(8):658-664.

12. Benet A, Prevedello DM, Carrau RL, et al. Comparative analysis of the transcranial "far lateral" and endoscopic endonasal "far medial" approaches: surgical anatomy and clinical illustration. *World Neurosurg*. 2014;81(2):385-396.

13. Fraser JF, Nyquist GG, Moore N, Anand VK, Schwartz TH. Endoscopic endonasal transclival resection of chordomas: operative technique, clinical outcome, and review of the literature. *J Neurosurg*. 2010;112(5):1061-1069.

14. Karam YR, Menezes AH, Traynelis VC. Posterolateral approaches to the craniovertebral junction. *Neurosurgery*. 2010;66(3)(suppl):135-140.

15. Wu A, Zabramski JM, Jittapiromsak P, Wallace RC, Spetzler RF, Preul MC. Quantitative analysis of variants of the far-lateral approach: condylar fossa and transcondylar exposures. *Neurosurgery*. 2010;66(6)(suppl):191-198.

16. Cappabianca P, Cavallo LM, Esposito F, De Divitiis O, Messina A, De Divitiis E. Extended endoscopic endonasal approach to the midline skull base: the evolving role of transsphenoidal surgery. *Adv Tech Stand Neurosurg*. 2008;33:151-199.

17. de Divitiis E. Endoscopic endonasal transsphenoidal surgery: from the pituitary fossa to the midline cranial base. *World Neurosurg*. 2013;80(5):e45-e51.

18. Kassam A, Snyderman CH, Mintz A, Gardner P, Carrau RL. Expanded endonasal approach: the rostrocaudal axis. part II; posterior clinoids to the foramen magnum. *Neurosurg Focus*. 2005;19(1):E4.

19. Morera VA, Fernandez-Miranda JC, Prevedello DM, et al. "Far-medial" expanded endonasal approach to the inferior third of the clivus: the transcondylar and transjugular tubercle approaches. *Neurosurgery*. 2010;66(6)(suppl):211-219.

20. Simal-Julián JA, Miranda-Lloret P, Beltrán-Giner A, Plaza-Ramirez E, Botella-Asunción C. Full endoscopic endonasal extreme far-medial approach: eustachian tube transposition. *J Neurosurg Pediatr*. 2013;11(5):584-590.

21. Alfieri A, Jho HD, Tschabitscher M. Endoscopic endonasal approach to the ventral cranio-cervical junction: anatomical study. *Acta Neurochir (Wien)*. 2002;144(3):219-225.

22. Cappabianca P, Alfieri A, Colao A, et al. Endoscopic endonasal transsphenoidal surgery in recurrent and residual pituitary adenomas: technical note. *Minim Invasive Neurosurg*. 2000;43(1):38-43.

23. Carrau RL, Jho HD, Ko Y. Transnasal-transsphenoidal endoscopic surgery of the pituitary gland. *Laryngoscope*. 1996;106(7):914-918.

24. Cavallo LM, Messina A, Cappabianca P, et al. Endoscopic endonasal surgery of the midline skull base: anatomical study and clinical considerations. *Neurosurg Focus*. 2005;19(1):E2.

25. Kassam A, Snyderman CH, Mintz A, Gardner P, Carrau RL. Expanded endonasal approach: the rostrocaudal axis, part I: crista galli to the sella turcica. *Neurosurg Focus*. 2005;19(1):E3.

26. Robinson S, Patel N, Wormald PJ. Endoscopic management of benign tumors extending into the infratemporal fossa: a two-surgeon transnasal approach. *Laryngoscope*. 2005;115(10):1818-1822.

27. Fernandez-Miranda JC, Morera VA, Snyderman CH, Gardner P. Endoscopic endonasal transclival approach to the jugular tubercle. *Neurosurgery*. 2012;71(1)(suppl):146-158.

28. Kassam AB, Vescan AD, Carrau RL, et al. Expanded endonasal approach: vidian canal as a landmark to the petrous internal carotid artery. *J Neurosurg*. 2008;108(1):177-183.

29. Yousry I, Moriggl B, Schmid UD, et al. Detailed anatomy of the intracranial segment of the hypoglossal nerve: neurovascular relationships and landmarks on magnetic resonance imaging sequences. *J Neurosurg*. 2002;96(6):1113-1122.

30. Hadad G, Bassagasteguy L, Carrau RL, et al. A novel reconstructive technique after endoscopic expanded endonasal approaches: vascular pedicle nasoseptal flap. *Laryngoscope*. 2006;116(10):1882-1886.

31. Kassam A, Carrau RL, Snyderman CH, Gardner P, Mintz A. Evolution of reconstructive techniques following endoscopic expanded endonasal approaches. *Neurosurg Focus*. 2005;19(1):E8.

32. Kassam AB, Prevedello DM, Carrau RL, et al. Endoscopic endonasal skull base surgery: analysis of complications in the authors' initial 800 patients. *J Neurosurg*. 2011;114(6):1544-1568.

33. Rivera-Serrano CM, Snyderman CH, Gardner P, et al. Nasoseptal "rescue" flap: a novel modification of the nasoseptal flap technique for pituitary surgery. *Laryngoscope*. 2011;121(5):990-993.

34. Zanation AM, Snyderman CH, Carrau RL, Kassam AB, Gardner PA, Prevedello DM. Minimally invasive endoscopic pericranial flap: a new method for endonasal skull base reconstruction. *Laryngoscope*. 2009;119(1):13-18.

35. Perez-Orribo L, Little AS, Lefevre RD, et al. Biomechanical evaluation of the craniovertebral junction after anterior unilateral condylectomy: implications for endoscopic endonasal approaches to the cranial base. *Neurosurgery*. 2013;72(6):1021-1029.

36. Vishteh AG, Crawford NR, Melton MS, Spetzler RF, Sonntag VK, Dickman CA. Stability of the craniovertebral junction after unilateral occipital condyle resection: a biomechanical study. *J Neurosurg*. 1999;90(1)(suppl):91-98.

37. Ciappetta P, Occhiogrosso G, Luzzi S, D'Urso PI, Garribba AP. Jugular tubercle and vertebral artery/posterior inferior cerebellar artery anatomic relationship: a 3-dimensional angiography computed tomography anthropometric study. *Neurosurgery*. 2009;64(5)(suppl 2):429-436.